

A FREE DRIFT MODEL FOR RIVER ICE COVER FORMATION

Chin Feng Ho and Hung Tao Shen

Department of Civil and Environmental Engineering
Clarkson University
Potsdam, New York 13676

ABSTRACT

In this study, a two-dimensional computer model for simulating the process of river ice cover formation is developed, and applied to a reach of the upper St. Lawrence River. The simulation model consists of the simulation of flow distribution using a stream-tube model, the simulation of water temperature and ice concentration distribution, the simulation of border ice formation and ice cover progression along with the ice cover thickness distribution. A free-drift model is used in simulating the ice movement. A comparison of the simulated results with the available field data shows that the model is capable of providing a good simulation. Further refinements by considering the internal ice resistance for the surface ice transport is needed.

INTRODUCTION

In the last two decades there have been many theories developed to describe river ice formation processes (Ashton, 1980; Michel, 1984; Shen, 1985). Computer models for simulating flow and ice conditions in rivers have been developed based on these theories. These models include quasi-steady state flow models developed by Petryk, et al (1981), Michel and Drouin (1981), Calkins (1984), and an unsteady flow model by Shen and Yapa (1984). All of these models are one-dimensional, which simulate only the cross-sectional average characteristics of flow and ice conditions. In a natural river, flow depth, velocity and ice thickness vary considerably across the width as observed in the field (Shen, et al. 1984). It is obvious that by taking into consideration the transverse variations in the analysis, a better understanding on the ice cover formation processes can be achieved. In this paper, the preliminary development of a two-dimensional simulation model for a reach of the upper St. Lawrence River is presented. Refinements which can be obtained by including the internal resistance of the surface ice layer, the effect of the vertical distribution and undercover accumulation of frazil suspension and the local effect of leading edge on ice transport are discussed.

FORMATION OF RIVER ICE COVER

As winter begins, large quantities of ice are produced and transported along the river in the form of frazil ice suspension. Frazil particles that are brought into contact with the river bed by the turbulence action may attach to the bed to form anchor ice. A significant portion of the frazil suspension will rise to the surface to form a moving layer of ice consisting of mixtures of slush, pans, and floes. For a uniform channel, the distribution of ice suspension over the flow depth and along the channel may be described by the following equation:

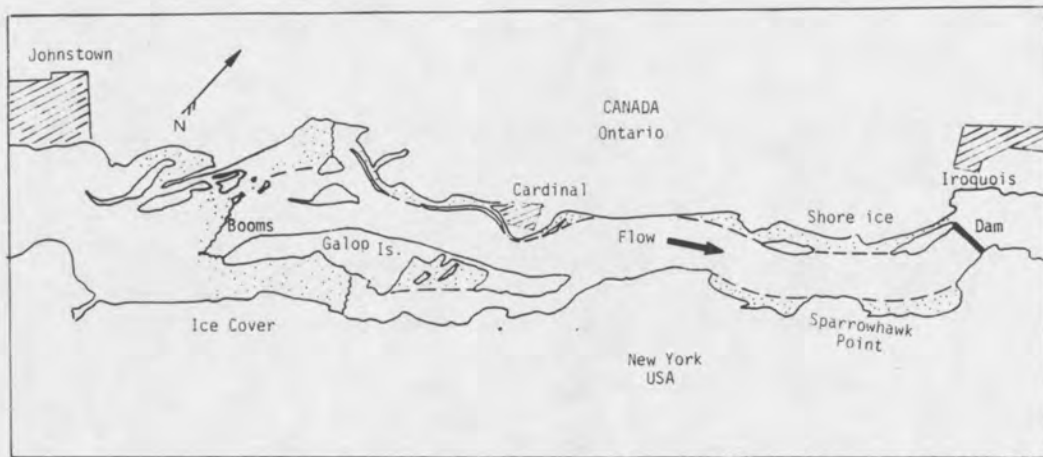


Figure 1: The Study Reach at the Time of the Main Ice Cover Formation

$$\frac{\partial C}{\partial t} + u \frac{\partial C}{\partial s} + v_b \frac{\partial C}{\partial z} = \frac{\partial}{\partial z} \left(\varepsilon_z \frac{\partial C}{\partial z} \right) + \Sigma \Phi \quad (1)$$

in which s, z = longitudinal and vertical coordinates; t = time; C = concentration of the ice suspension; u = longitudinal velocity; v_b = buoyant velocity of ice particles; ε_z = vertical mixing coefficient; $\Sigma \Phi$ = the rate of net heat loss per unit volume. In Eq. 1, the rise of frazil ice suspension is affected by the combined effect of the buoyant velocity and the vertical turbulent mixing. The rise of frazil ice to the surface of the river will either increase the area concentration of the surface layer, or attached to the bottom of the surface ice floes to increase their thickness. Both increases in the thickness and the area concentration of the surface ice may lead to reduction in surface heat loss, and hence the ice production. During the ice cover formation period, the moving surface ice layer will accumulate against an artificial obstacle or a natural ice bridge leading to the upstream progression of the surface ice cover. The ice remaining in the suspension will continue to be transported under the ice cover, and gradually rise to the underside of the ice cover to be transported along the cover or accumulate into hanging dams.

SIMULATION OF ICE TRANSPORT AND ACCUMULATION

In this section the development of a two-dimensional simulation of ice cover progression in the 4.4-mile (7 km.) reach of the St. Lawrence River between Cardinal and Iroquois Control Dam as shown in Fig. 1 is discussed. The slope of this reach varies approximately from 2×10^{-5} during the open water condition to 5×10^{-5} after the initial ice cover formation. The average depth of flow is in the order of 33 feet (10 m.).

Computer Simulation

For the purpose of simulation, the study reach is schematized into 52 sub-reaches connected by 53 cross-sections. Each cross-section is sub-divided into 20 streamtubes of equal discharge. The basic data required for performing the hydraulics computation are cross-section geometry, sub-reach lengths, bed and ice cover roughness, downstream boundary elevation, and discharge. Additional data required for thermal-ice calculations are the water temperature or the ice concentration at the upstream boundary, and the air temperature. Major processes to be simulated for the formation of ice cover include distributions of water temperature or ice concentration, border ice formation, ice cover progression, and thickness distribution.

River hydraulics computation. - Flow conditions in the river for each time step are computed by a standard

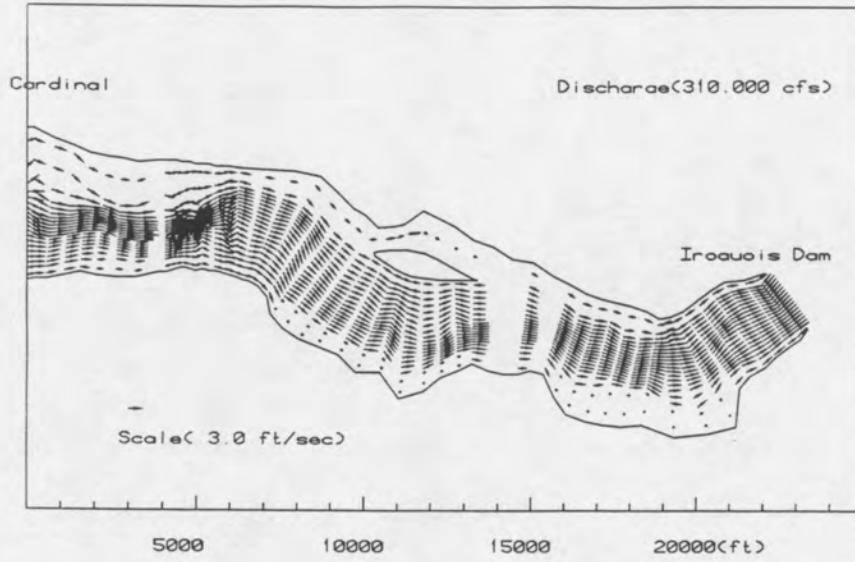


Figure 2: Flow Distribution at Selected Cross-Sections

step backwater method for composite channels (Henderson, 1966), with modifications to include the ice cover effect and the transverse flow distribution. In ice covered regions the composite Manning's coefficient, n_c , is computed by the Beloken-Sabaneev formula (Uzuner, 1975).

$$n_c = \left[(n_i^{2/3} + n_b^{2/3}) / 2 \right]^{2/3} \quad (2)$$

in which, n_b and n_i = Manning's coefficients of the channel bed and the ice cover, respectively. The transverse flow distribution in a channel cross-section is computed using Eq. 3.

$$q_p = Q (A_p R_p^{2/3} / \sum_{n=1}^{20} A_n R_n^{2/3}) \quad (3)$$

in which, q_p = discharge in the pth element, with area A_p and hydraulic radius R_p ; Q = river discharge; A_n = area of the nth element; R_n = hydraulic radius of the nth element. Fig. 2 shows an example of computed velocity distribution at the 53 selected cross-sections. Fig. 3 shows the velocity distribution on an Eulerian grid system interpolated from the distribution in Fig. 2.

Simulation of ice concentration distribution. - The distribution of depth-averaged water temperature, T_w , is computed from

$$\frac{\partial T_w}{\partial t} + \vec{v} \cdot \nabla T_w = \frac{B h_{wa} (T_w - T_a)}{\rho C_p A} \quad (4)$$

in which, h_{wa} = heat exchange coefficient at the air-water interface, $22.4 W m^{-2} C^{-1}$; T_a = air temperature; \vec{v} = velocity; B = top width of the open water area; A = flow cross-section area; ρ = water density; and C_p = specific heat of water. When the water temperature reaches the freezing point, the frazil concentration, C_i , can be calculated from

$$\frac{\partial C_i}{\partial t} + \vec{v} \cdot \nabla C_i = \frac{B h_{wa} (T_f - T_a)}{\rho_i L_i A} + S_i \quad (5)$$

in which, T_f = freezing point, $0^\circ C$; ρ_i = density of ice; S_i = a source/sink term which represents the deposition and erosion of frazil ice, and L_i = latent heat of fusion of ice. Considering that $Q_i \ll Q$ the total ice discharge at a river cross-section is approximated by $Q_i = Q C_i$. A fraction of Q_i will contribute

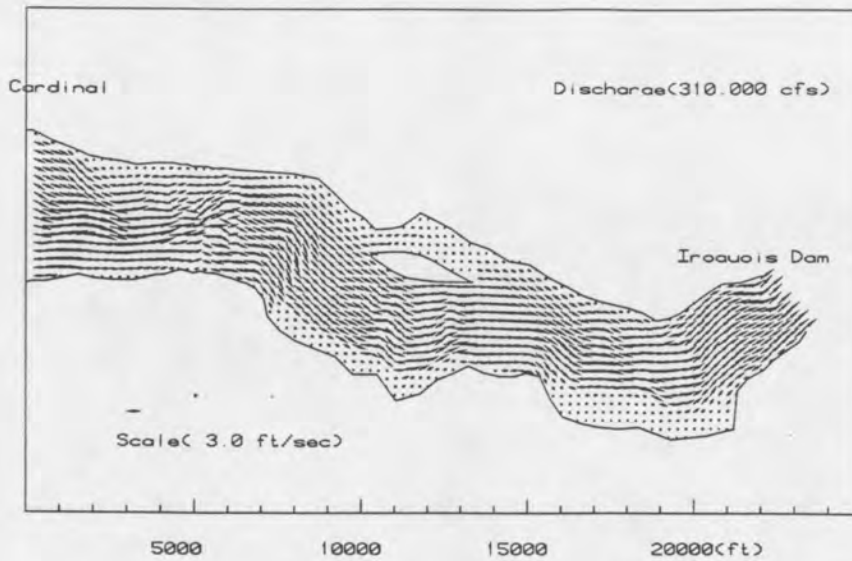


Figure 3: Flow Distribution on Finite Difference Grids

to the surface ice discharge Q_i^s , which supplies the ice for ice cover formation. The ratio $\alpha_s = Q_i^s/Q_i$ may vary with the travel distance, flow velocity, turbulence level, and the weather condition. Eqs. 4 and 5 are solved numerically using a Lagrangian-Eulerian scheme. In this scheme, the displacement of ice mass (water mass in the case of Eq. 4) in each Eulerian grid during a time step is calculated by numerically integrating the drift velocity \vec{v} over the time interval. Fig. 4 shows typical trajectories of ice elements released at the upstream boundary during a three hour period. The change in ice mass due to the heat exchange is accounted for at the end of each time step. Fig. 5 shows an example of the simulated ice concentration distribution in the study reach at the end of a 4 hour simulation. Fig. 6 shows a similar simulation by neglecting the ice production due to surface heat exchanges. In the preceding discussion, free drift was assumed for the movement of ice elements. Further improvement by considering the forces acting on the ice element can be made by using the following equation of motion for the surface ice.

$$M_i \frac{d\vec{v}_i}{dt} = \vec{R} + \Sigma \vec{F} \quad (6)$$

in which, M_i = ice mass per unit area, \vec{R} = internal ice resistance, $\Sigma \vec{F}$ = external forces including gravity, wind drag and current drag.

Border Ice Formation. - Border ice formation is an important component in the ice cover formation process. The formation of border ice can reduce the amount of ice production, alter the distribution of flow across the channel, and affect the surface ice transport capacity of the river. All of these can have significant influences on the formation of ice bridges and the rate of progression of ice cover. In extreme low velocity regions, border ice can form statically through local surface heat exchange (Matousek 1984). Beyond these regions, border ice can form through the hydraulic accumulation of surface ice particles travelling along the river in contact with the river bank or the boundary of existing border ice. Several studies (Michel, et al. 1982, Shen et al., 1984, Hirayama 1986) used the limiting velocity criteria for this type of border ice growth with reasonable success. In general, however, the growth of border ice through hydraulic accumulation should be considered as the result of the dynamic transport of surface ice elements along the border. The movement of surface ice particles along the border, which can be analytically represented by Eq. 6, are driven by the gravity force, wind and water drags, and stresses imposed by neighboring ice particles. When the tangential component of the resultant of these driving forces are smaller than the resisting frictional

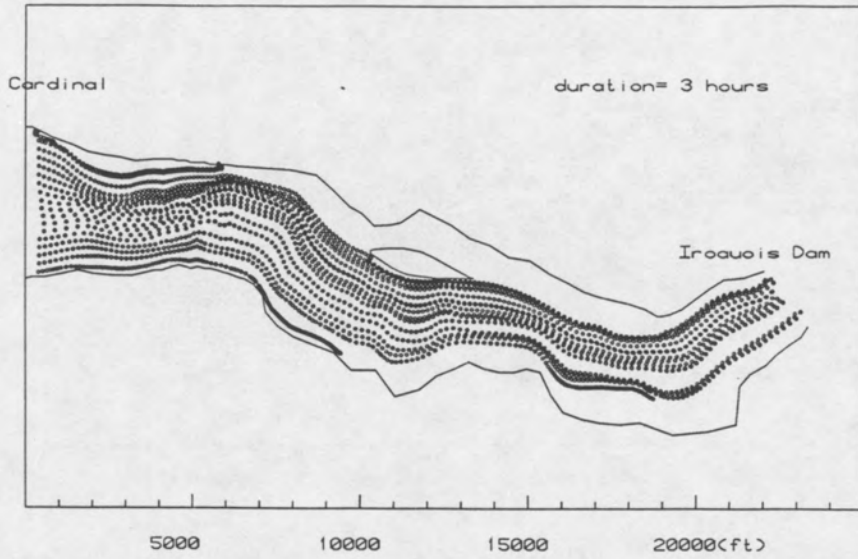


Figure 4: Trajectories of Ice Particles

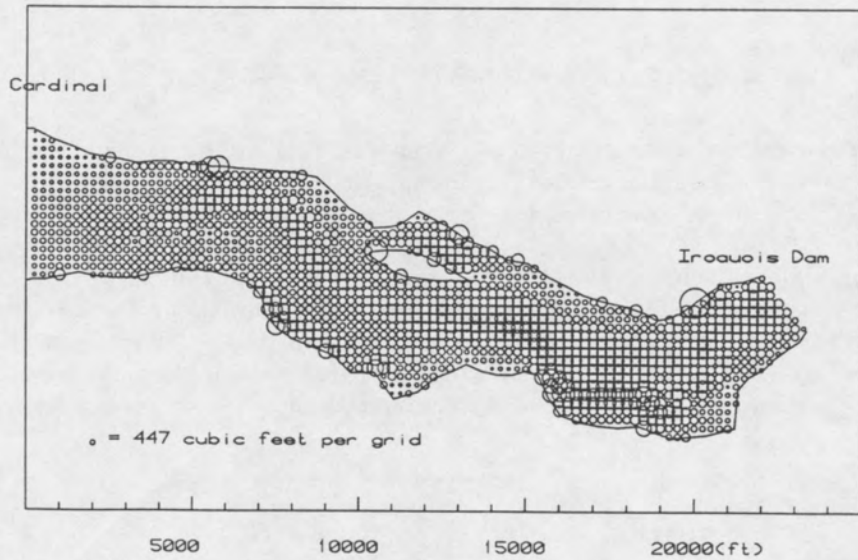


Figure 5: Simulated Ice Concentration Distribution

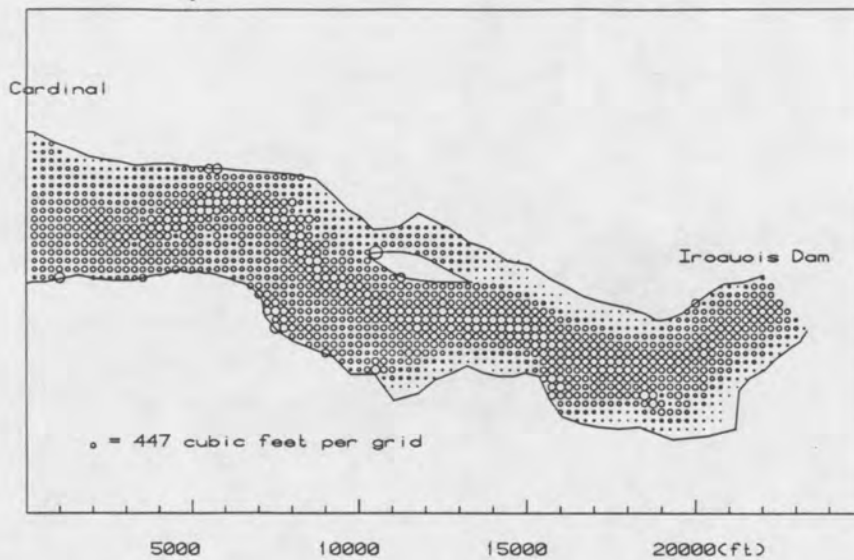


Figure 6: Simulated Ice Concentration Distribution, Neglecting Ice Productions

force along the border, the surface ice will attach to the border to increase the width of the border ice. The frictional force should be related to the normal component of the resultant force and the ice cohesion. In addition to the above considerations, the hydrodynamic stability of ice particles should also be considered. In cases where the flow velocity normal to the existing border ice is relatively large, the overturning of ice particles can limit the lateral progression of the border ice. Since the free-drift model can not consider the dynamics of ice particles, a simplified kinematic formulation is used. In the present model, the shore ice growth is limited by the following conditions:

$$V_t \leq 0.70 \text{ fps} (0.213 \text{ m/s}) \quad \text{and} \quad F_{rn} = \frac{V_n}{\sqrt{gh}} \leq 0.05 \quad (7)$$

in which, V_t and V_n = tangential and normal velocity components along the existing border ice boundary. The values given in Eq. 7 are site specific, since they are functions of channel slope, ice characteristics and weather conditions. Fig. 7 shows a comparison between observed and simulated border ice in the study reach.

Ice Cover Formation. - Since the ice cover in the study reach is initiated by dipping gates at the Iroquois Dam, the date on which gates were dipped is used as the time of cover initiation. The ice cover progression and thickness distribution are simulated based on existing ice jam theories (Pariset and Hausser 1961, Michel 1984, Tatinclaux 1977). Field observations indicated that shoving does not occur in the study reach. The narrow jam formula is used in the present simulation. The ice cover thickness h_i can be computed from

$$\frac{V}{\sqrt{gH}} = \left(1 - \frac{h_i}{H}\right) \sqrt{2(1 - e_c) \left(1 - \frac{\rho_i}{\rho}\right) \frac{h_i}{H}} \quad (8)$$

in which, V and H = local depth-averaged velocity and flow depth immediate upstream of the leading edge; $e_c = e_p + (1 - e_p)e$, porosity of the ice accumulation; e = porosity of individual ice floes; e_p = porosity of the ice accumulation between ice floes. The lower limit of ice cover thickness occurs when h_i is equal to the thickness of ice floe, t_i . At this condition, there exists a critical Froude number for the formation of ice cover by juxtaposition. Based on field observations (Shen et al., 1984), this critical Froude number

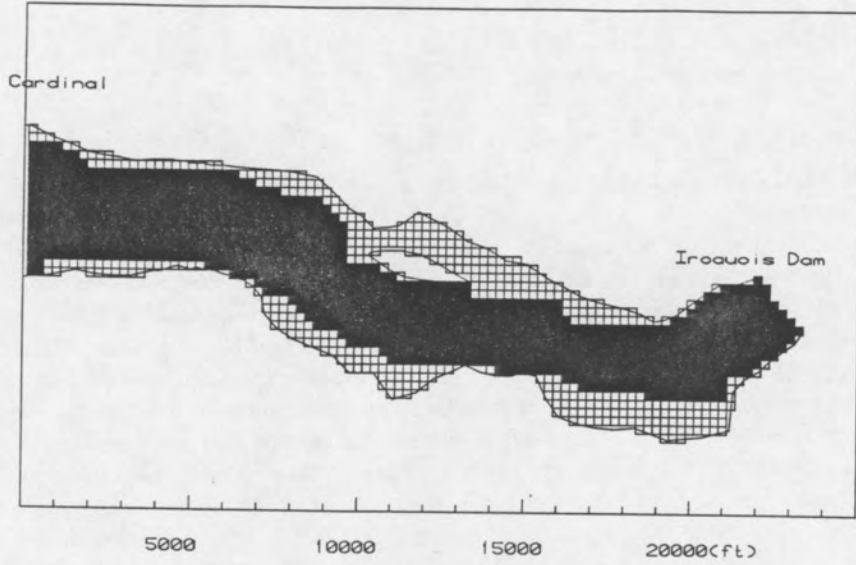


Figure 7: Comparison Between Simulated Border Ice and the Field Condition

is approximately equal to 0.05. The value of t_i is assumed to be 6 inches. From Eq. 8 one can also show that there is a maximum Froude number, which corresponds to the maximum h_i/H value, at which the ice cover can not progress. Based on field observations in various rivers, Kisvild (1959) indicated that this value can vary between 0.05 and 0.10. Analysis of the field data in the study reach for all winters between 1971 and 1984 (Ho 1986) indicated that the ice cover progression will stop when the maximum local Froude number at a cross-section falls in the range of 0.0916 to 0.0938. For $e = e_p = 0.39$, Eq. 8 gives a maximum Froude number 0.0927 and a corresponding h_i/H ratio of 0.33.

Based on the preceding discussion, the width-averaged ice cover progression distance, ΔL_c , during each time step can be calculated from the conservation of mass

$$\Delta L_c = \alpha_s Q_i \Delta t / (\sum_{k=1}^K h_i^k \cdot \Delta w) \quad (9)$$

in which, Δt = time interval; Δw = width of the element at the leading edge cross-section; k = index for elements in the cross-section.

Sample simulations. - Based on the formulation discussed, a computer model is developed to simulate the progression and the two-dimensional thickness distribution of the ice cover in the study reach. The variation of the coefficient α_s is obtained by calibrating against the field data. Figs. 8 and 9 show the air temperature and discharge during the ice cover formation period. The Manning's coefficients for the bed and the ice cover are 0.032 and 0.033, respectively. Fig. 10 compares the simulated and observed leading edge positions of the ice cover. The solid curve is simulated by assuming $e_c = 0.6$ and the dashed curve is simulated by assuming $e_c = 0.5$. Values of α_s used in the simulation are also indicated. This figure shows that the coefficient α_s is relatively low and decreases as the ice cover progressed upstream. The low α_s values may be due to the high concentration of surface ice which effectively reduces the heat exchange between air and water. The decrease in α_s along the river is considered to be due to the decrease in the distance between the frazil ice generation area and the leading edge of the ice cover. Fig. 10 also indicated that the value of α_s increases when the air temperature decreases. A plausible explanation is that the size and buoyant velocity of the frazil ice will be larger during frazil ice travelling to downstream, and frazil ice will be brought to the surface at a faster rate. The simulated initial ice cover thickness distribution at the cessation of the ice cover progression at Jan. 19, 1982 is presented in Fig. 11. A comparison of Fig. 11 with the river bed topography as shown in Fig. 12 show that the maximum ice cover thickness is located along the deepest region of the river bed, where the Froude number is the highest. This phenomena agrees with field observations (Shen et al. 1984).

SUMMARY AND DISCUSSIONS

In this study, a two-dimensional computer model for simulating the process of ice cover progression is developed for a reach of the St. Lawrence River. The simulation consists of four steps: the simulation of flow distribution, the simulation for water temperature and ice discharge, the simulation of border ice formation, and the simulation of the ice cover progression with two-dimensional cover thickness distribution. A comparison of the simulated results with the available data shows that the computation is capable of providing a good simulation in the ice cover progression and the ice cover thickness distribution, due to the accumulation of surface ice. The simulation results also show that thicker surface ice cover are formed in regions with large Froude number, which agrees with data obtained from field observations. Further refinements by considering the internal ice resistance is needed. In the field the leading edge of the ice cover often appear in the form of an irregular V-shape. This irregular leading edge can generate a strong transverse surface current which tends to funnel the surface ice supplies toward the apex of the leading edge. To improve the simulation capability of the model this phenomena should be considered, since it can affect the thickness distribution of the ice cover. In addition to the simulation of the surface ice accumulation the transport and deposition of suspended frazil ice should also be included in order to provide a complete description of the ice cover and hanging dam formation phenomena.

ACKNOWLEDGEMENTS

This study is supported in part by the U.S. Army Cold Regions Research and Engineering Laboratory under Contact No. DACA89-87-K-0001.

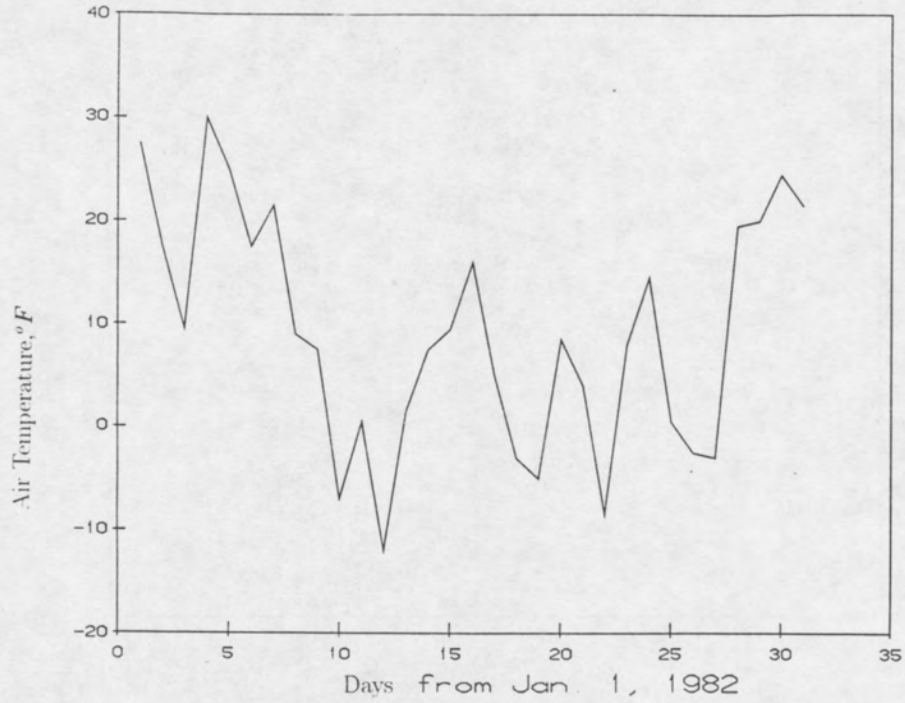


Figure 8: Air Temperature During Ice Cover Formation Periods

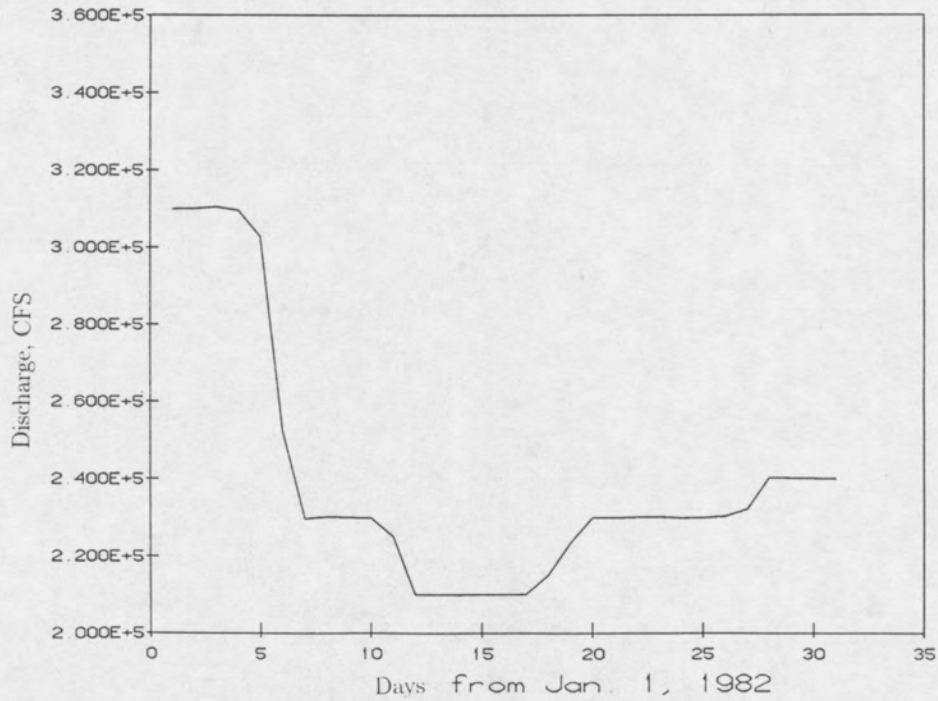


Figure 9: Discharge at the Iroquois Dam During Ice Cover Formation Period

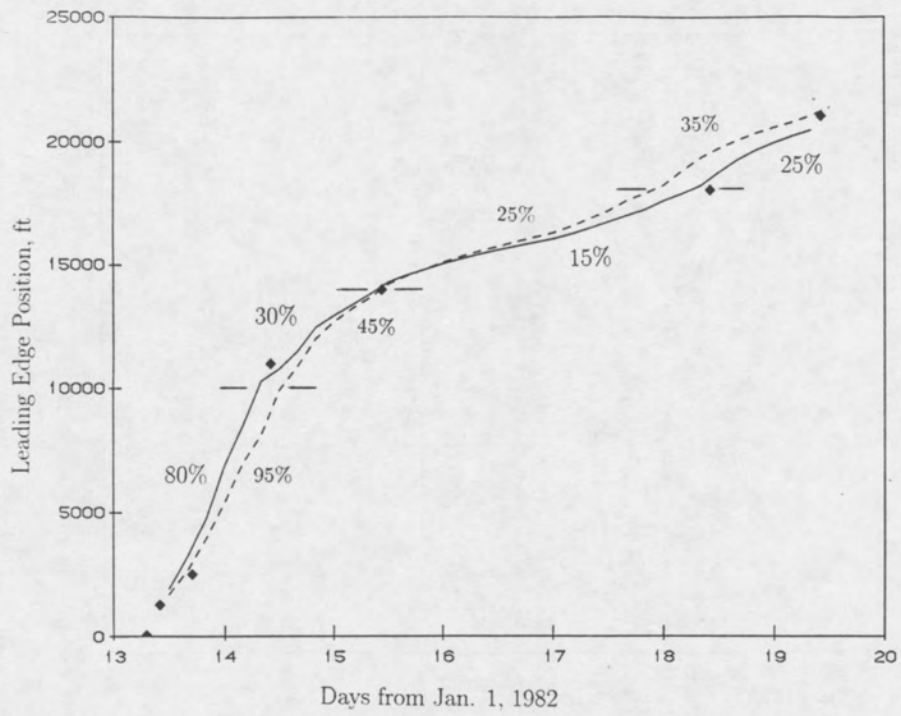


Figure 10: Comparison of Simulated and Observed Leading Edge Positions

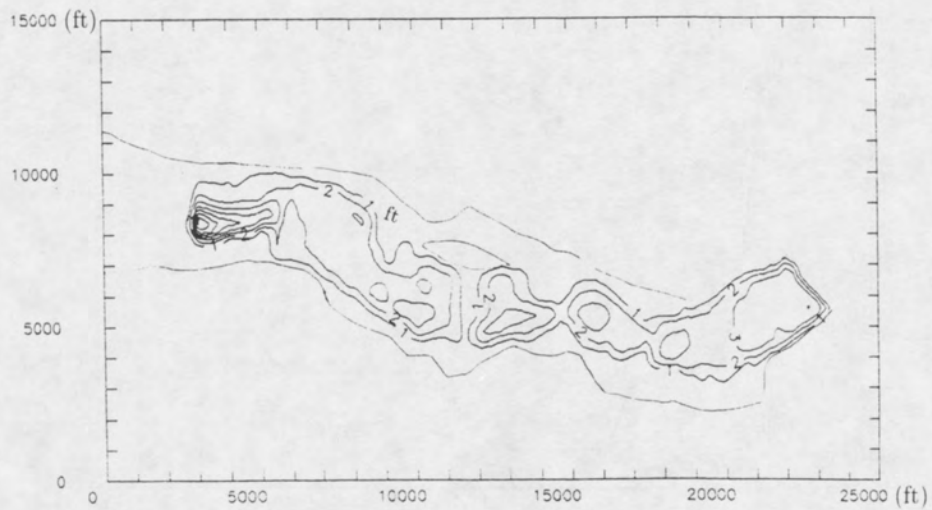


Figure 11: Simulated Initial Ice Cover Thickness



Flow →

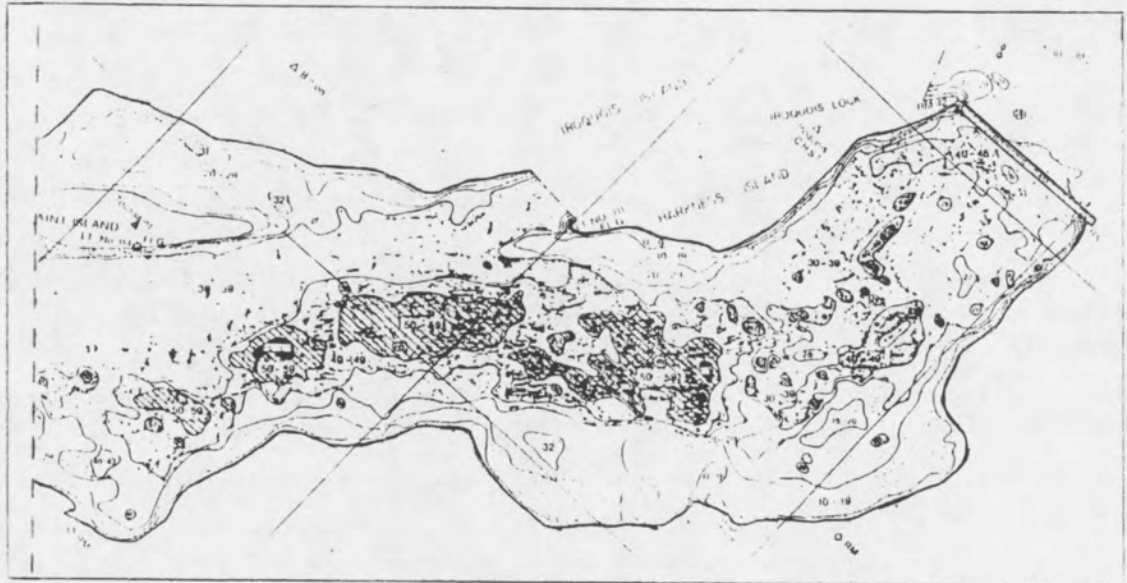


Figure 12: Channel Bottom Topography in the Study Reach

REFERENCES

- Ashton, G.D., 1980. "Freshwater Ice Growth, Motion and Decay," *Dynamics of Snow and Ice Masses*, S.C. Colebeck ed., Academic Press, pp. 261-304.
- Calkins, D.J., 1984. "Numerical Simulation of Freeze-up on the Ottawaquechee River," *Workshop on the Hydraulics of River Ice*, Fredericton, N.B., pp. 245-277.
- Hausser, R., Saucett, J.P., and Parkenson, F.E., 1984. "Coverage Coefficient for Calculating Ice Volume Generated," *Workshop on the Hydraulics of River Ice*, Fredericton, N.B., pp. 211-224.
- Henderson, F.M., 1966. "Open Channel Flow," Macmillan Company, New York.
- Hirayama, K., 1986. "Growth of Ice Cover in Steep and Small Rivers," *Proceedings, IAHR Symposium on Ice*, Iowa City, pp. 451-464.
- Ho, C.F., 1986. "Two-Dimensional Application of Ice Cover Progression Theories in a Large River," *M.S. Thesis*, Clarkson University, Potsdam, N.Y., 74p.
- Kivisild, H.R., 1959. "Hydrodynamical Analysis of Ice Floods," *8th IAHR Congress*, Paper 23 F, Montreal, Canada, pp. 23-F-1-30.
- Matoušek, V., 1984. "Types of Ice Run and Conditions for Their Formation," *Proceedings, IAHR Symposium on Ice*, Hamburg, pp. 316-327.
- Michel, B., 1984. "Comparison of Field Data with Theories on Ice Cover Progression in Large Rivers," *Canadian Journal of Civil Engineering*, Vol. 11, pp. 798-814.
- Michel, B., and Drouin, M., 1981. "Courbes de remous sous les couverts de glace de la Grande Riviere," *Canadian Journal of Civil Engineering*, Vol. 8, pp. 351-363.
- Pariset, E. and Hausser, R., 1961. "Formation and Evolution of Ice Covers on Rivers," *Transactions, Engineering Institute of Canada*, Vol. 5, No. 1, pp. 41-49.
- Petryk, S., Panu, U., Kartha, V.C., and Clement, F., 1981. "Numerical modelling and predictability of ice regime in rivers," *International Symposium on Ice, IAHR*, Quebec, Vol. 1, pp. 436-449.
- Shen, H.T., *Hydraulics of River Ice*, Report 85-1, Department of Civil and Environmental Engineering, Clarkson University, Potsdam, N.Y., 80p.
- Shen, H.T., VanDeValk, W.A., 1984. "Field Investigation of St. Lawrence River Hanging Ice Dams," *IAHR Ice Symposium*, Hamburg, pp. 242-250.
- Shen, T.H., Ruggles, R.W., and Batson, G.B., 1984. "Field Investigation of St. Lawrence River Hanging Ice Dams, Winter of 1983-84," Report DTSL55-84-C-C0085A, U.S. Department of Transportation, Washington, D.C., 85p.
- Shen, H.T., and Yapa, P.D., 1984. "Computer Simulation of Ice Cover Formation in the Upper St. Lawrence River," *Workshop on Hydraulics of River Ice*, Fredericton, N.B., pp. 227-246.
- Tatinclaux, J.-C., 1977. "Equilibrium Thickness of Ice Jams," *Journal of the Hydraulics Division, ASCE*, Vol. 103, No. H69, pp. 959-974.
- Uzuner, M.S., 1975. "The Composite Roughness of Ice Covered Streams," *Journal of Hydraulic Research*, Vol. 13, No. 1, pp. 79-101.
- Wigle, T.E. and Bartholomew, J., 1981. "Winter Operations International Rapids Section on the St. Lawrence River," *International Symposium on Ice, IAHR*, Quebec, Vol. 1, pp. 193-210.